Supporting Information

$(NH_4)_2AgX_3$ (X=Br, I): 1D Silver Halides with Broadband White Light Emission and Improved Stability

*Tielyr D. Creason,[1†] Hadiah Fattal,[1†] Isaiah W. Gilley, [1] Timothy M. McWhorter,[1] Mao-Hua Du,[2] Bayram Saparov[1]**

[1]Department of Chemistry and Biochemistry, University of Oklahoma, 101 Stephenson Parkway, Norman, OK 73019, United States

[2]Materials Science & Technology Division, Oak Ridge National Laboratory, Oak Ridge, Tennessee 37830, United States

*Corresponding Author: saparov@ou.edu

[†]These authors contributed equally.

Table S1. Selected single crystal data and structure refinement parameters for $(NH_4)_2AgBr_3$ and $(NH_4)_2AgI_3$.

Formula	**$(NH_4)_2AgBr_3$**	**$(NH_4)_2AgI_3$**
Formula weight (g/mol)	383.68	524.65
Temperature (K)	295(2)	
Radiation, wavelength (Å)	Mo Kα, 0.71073	
Crystal system	Orthorhombic	
Space group	*Pnma*	
Z	4	
Unit cell parameters (Å)	a = 9.5890(3)	a = 10.1968(16)
	b = 4.5949(2)	b = 4.8347(7)
	c = 18.5212(6)	c = 19.847(4)
Volume (Å^3)	816.05(5)	978.4(3)
Density (ρ_{calc}) (g/cm^3)	3.123	3.562
Absorption coefficient (μ) (mm^{-1})	17.060	11.445
$\theta_{min} - \theta_{max}$ (º)	3.93 – 32.50	2.864 – 30.603
Reflections collected	18128	18780
Independent reflections	1796	1514
R^a indices ($I > 2\sigma(I)$)	R_1 = 0.0275	R_1 = 0.0202
	wR_2 = 0.0507	wR_2 = 0.0389
Goodness-of-fit on F^2	1.006	1.069
Largest diff. peak and hole (e$^-$/Å^3)	1.511 and -1.468	1.535 and -1.183

[a] $R_1 = \sum||F_0| - |F_c||/\sum|F_0|$; $WR_2 = |\Sigma|w(F_0^2 - F_c^2)^2/\sum|wF_0^2{}^2|^{1/2}$,

where $w = 1/|\sigma^2F_0^2 + (AP)^2 + BP|$, with $P = (F_0^2 + 2F_c^2)/3$ and weight coefficients A and B

Table S2. Atomic coordinates and equivalent isotropic displacement parameters (U_{eq}[a]) for $(NH_4)_2AgBr_3$ and $(NH_4)_2AgI_3$.

Atom	*x*	*y*	*z*	U_{eq}, Å^2
		$(NH_4)_2AgBr_3$		
N1	0.2438(4)	0.250000	0.5426(2)	0.0385(8)
N2	0.5731(4)	0.250000	0.2119(2)	0.0371(8)
Ag	0.37369(4)	0.750000	0.36795(2)	0.04454(11)
Br1	0.50543(5)	0.250000	0.40239(3)	0.03634(11)
Br2	0.11781(4)	0.750000	0.42793(2)	0.03461(11)
Br3	0.30945(5)	0.750000	0.22524(2)	0.03436(11)
		$(NH_4)_2AgI_3$		
N1	0.0743(4)	0.250000	0.7110(2)	0.0432(10)
N2	0.2519(5)	0.250000	0.4577(2)	0.0457(10)
Ag	0.36573(4)	0.750000	0.63506(2)	0.04790(11)
I1	0.50037(3)	0.250000	0.60023(2)	0.03764(9)
I2	0.30864(3)	0.750000	0.77602(2)	0.03687(9)
I3	0.11746(3)	0.750000	0.57080(2)	0.03735(9)

[a]*U*eq is defined as one-third of the trace of the orthogonalized *Uij* tensor.

Table S3. A comparison of bond distances and angles within the 1D $^{1}_{\infty}[AgX_3]^{2-}$ chains in $(NH_4)_2AgBr_3$ and $(NH_4)_2AgI_3$.

Atom pair	Distance (Å)	Label	Angle (°)
$(NH_4)_2AgBr_3$			
Ag – Br1 (×2)	2.6983(3)	Br1-Ag-Br2	109.207(14)
Ag – Br2	2.6934(3)	Br1-Ag-Br3	109.664(14)
Ag – Br3	2.7139(6)	Br2-Ag-Br3	101.239(19)
$(NH_4)_2AgI_3$			
Ag – I1 (×2)	2.8647(4)	I1-Ag-I2	109.505(12)
Ag – I2	2.8576(8)	I1-Ag-I3	108.630(14)
Ag – I3	2.8345(7)	I2-Ag-I3	104.982(19)

Table S4. Summary of time-resolved photoluminescence (TRPL) refinement parameters for $(NH_4)_2AgBr_3$ and $(NH_4)_2AgI_3$.

Parameter	**$(NH_4)_2AgBr_3$**	**$(NH_4)_2AgI_3$**
A_1 (Cnts)	532.3859	62.81477
τ_1 (μs)	0.521073 μs	5.994375 μs
A_2 (Cnts)	72.95995	434.3554
τ_2 (μs)	4.455118μs	0.5617258 μs
Average lifetime	0.995 μs	1.25 μs

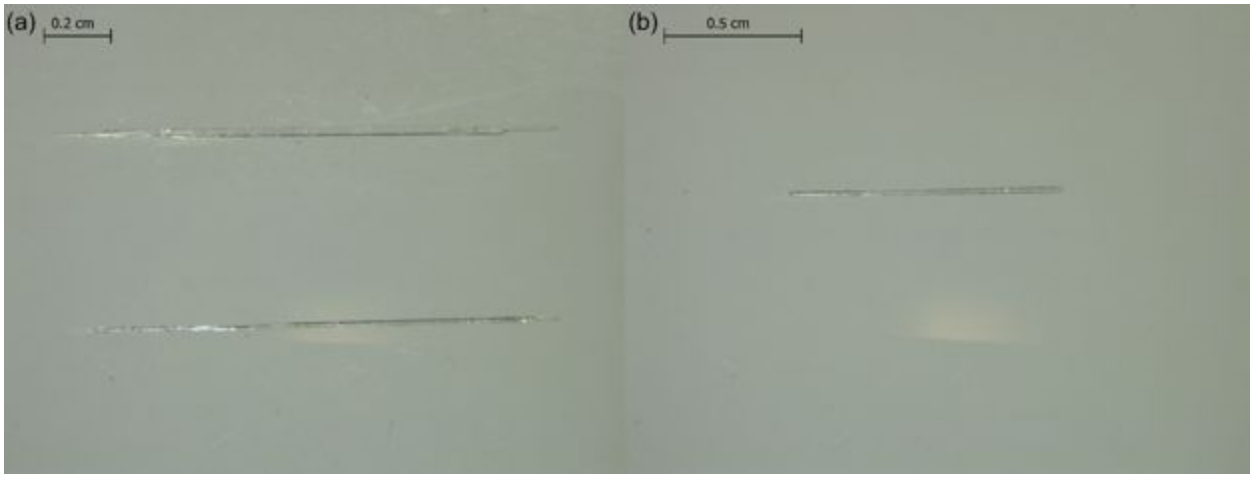

Figure S1. Photographs of (a) $(NH_4)_2AgBr_3$ and (b) $(NH_4)_2AgI_3$ single crystals grown via hydrothermal synthesis method.

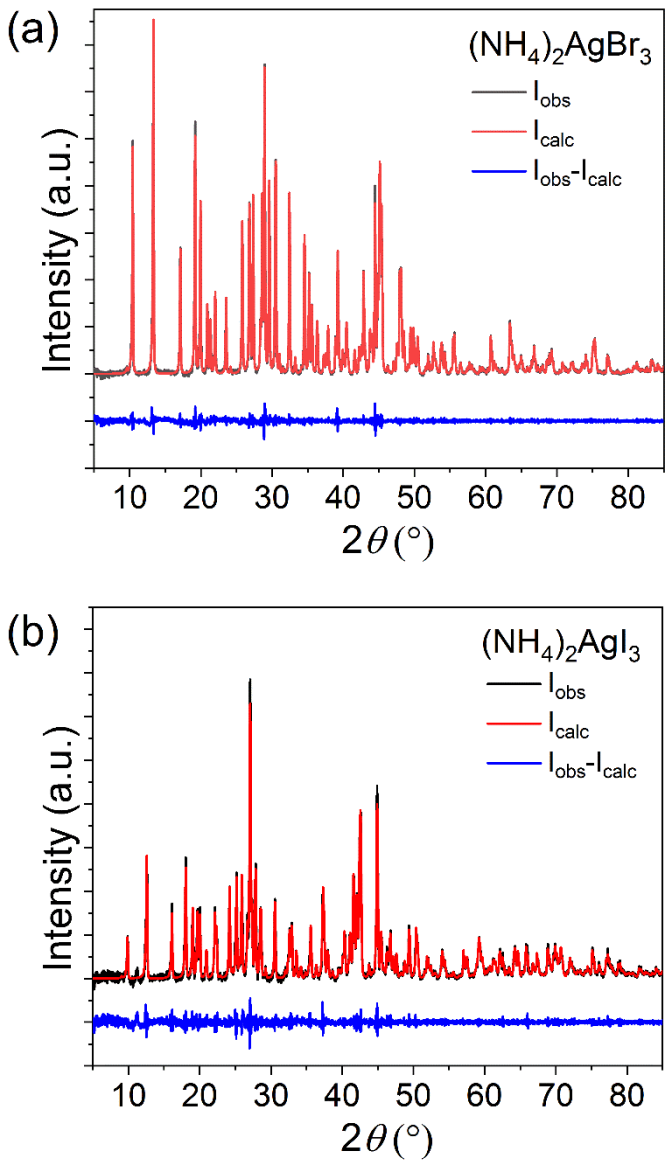

Figure S2. Room temperature PXRD patterns (black) fitted using the Pawley method (red) for (a) $(NH_4)_2AgBr_3$ and (b) $(NH_4)_2AgI_3$ prepared through hydrothermal synthesis.

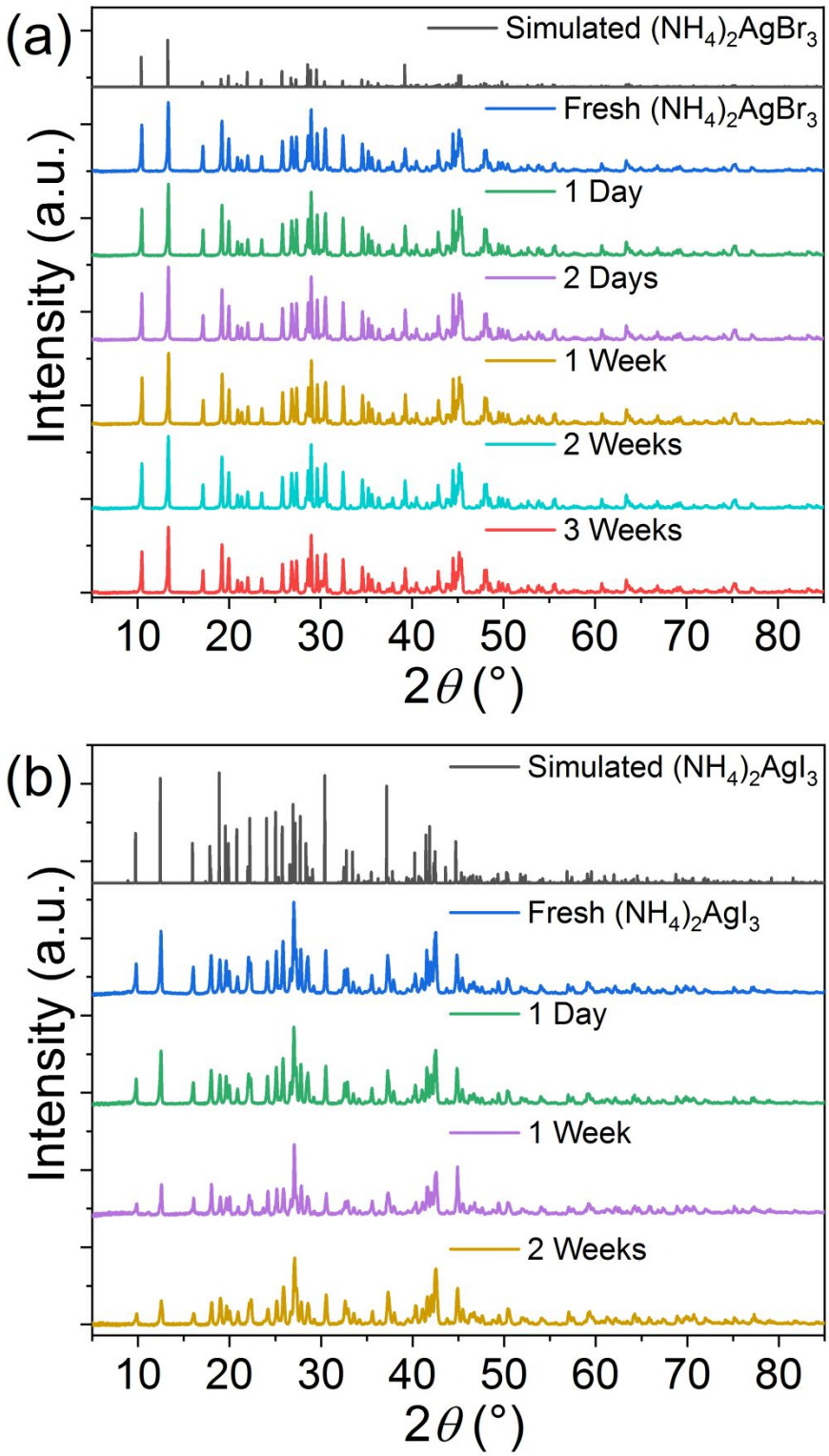

Figure S3. PXRD patterns of polycrystalline samples of (a) $(NH_4)_2AgBr_3$ and (b) $(NH_4)_2AgI_3$ left in ambient air for 3 weeks.

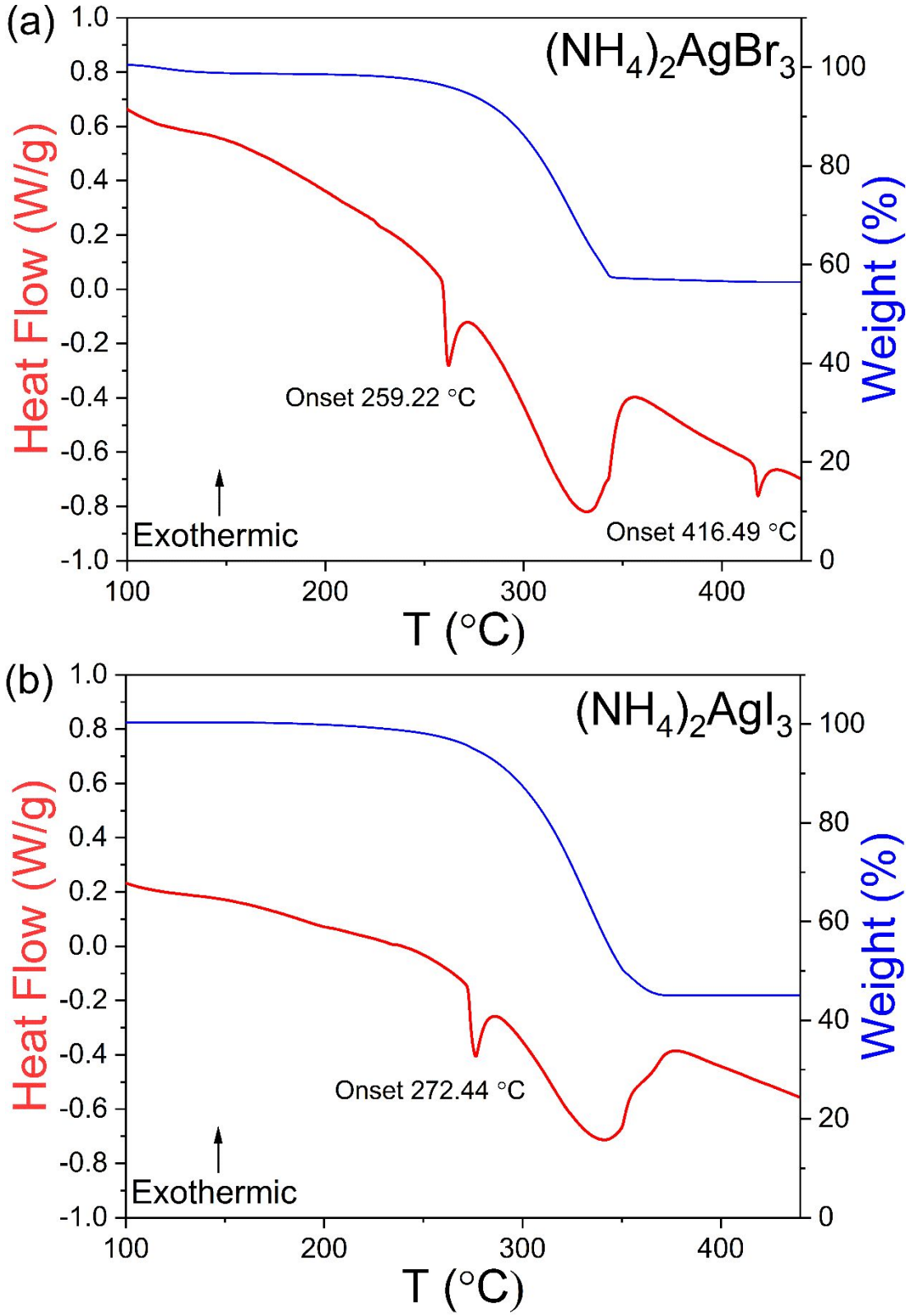

Figure S4. Differential scanning calorimetry (DSC, in red) and thermogravimetric analysis (TGA, in blue) plots for (a) $(NH_4)_2AgBr_3$ and (b) $(NH_4)_2AgI_3$.

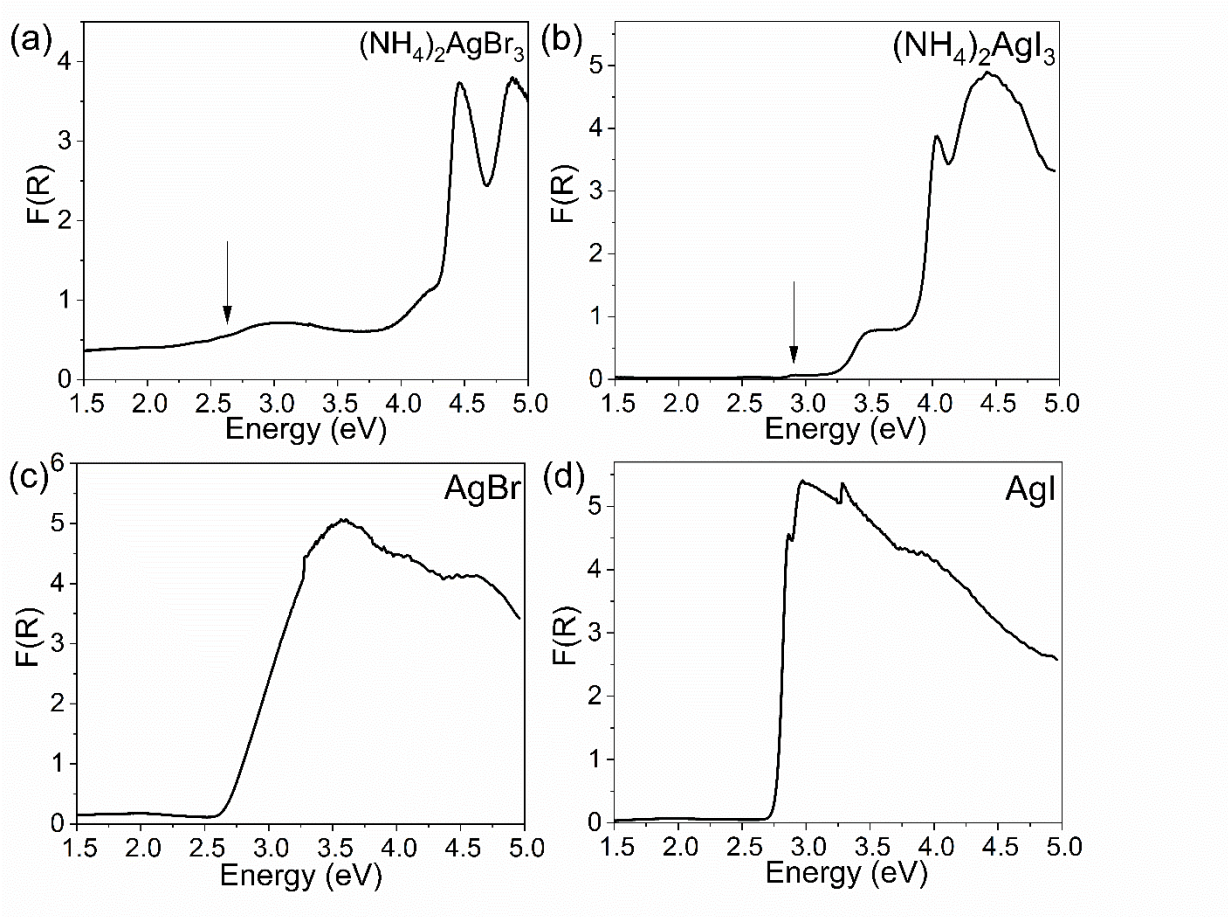

Figure S5. Kubelka-Munk transformed diffuse reflectance plots for (a) $(NH_4)_2AgBr_3$, (b) $(NH_4)_2AgI_3$, (c) AgBr, and (d) AgI. Arrows indicate minor impurities of AgX in $(NH_4)_2AgX_3$.

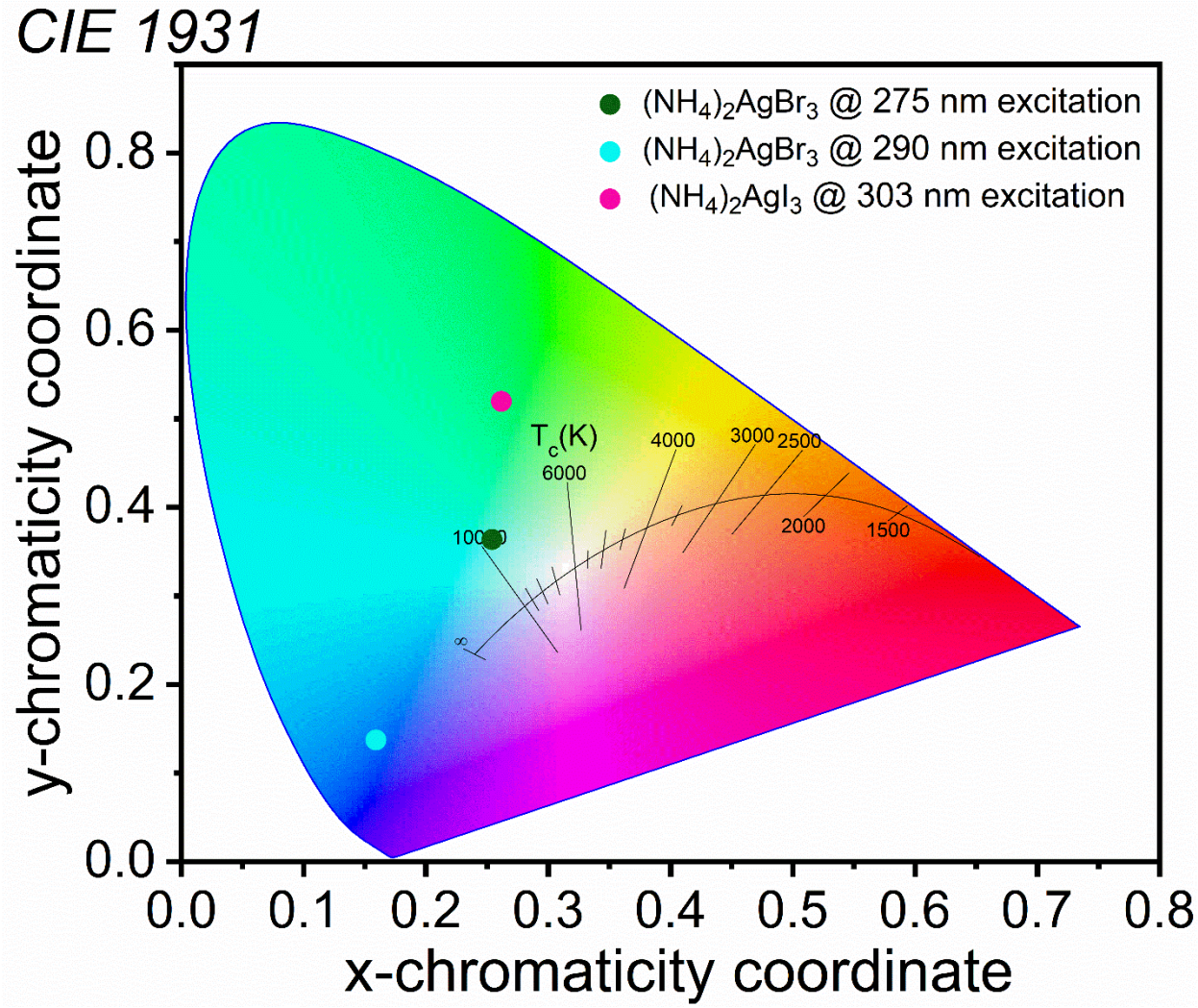

Figure S6. The Commission Internationale de l'Eclairage (CIE) color coordinates of $(NH_4)_2AgBr_3$ and $(NH_4)_2AgI_3$. $(NH_4)_2AgBr_3$ is found to exhibit excitation-dependent light emission properties. A Planckian locus has been included to estimate correlated color temperature (CCT) for the various PL emissions of $(NH_4)_2AgX_3$.

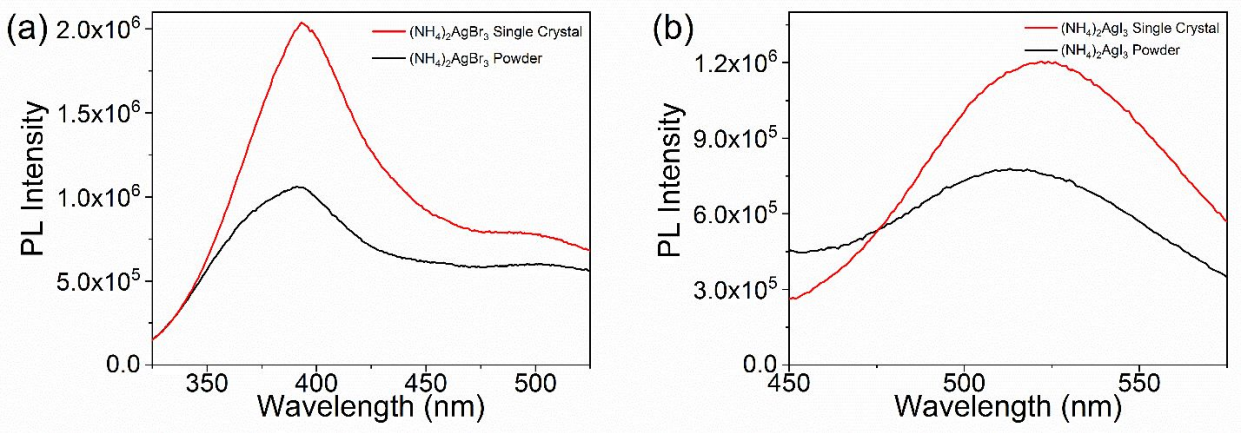

Figure S7. Comparisons of PL emission from single crystals and polycrystalline powders of (a) $(NH_4)_2AgBr_3$ and (b) $(NH_4)_2AgI_3$.

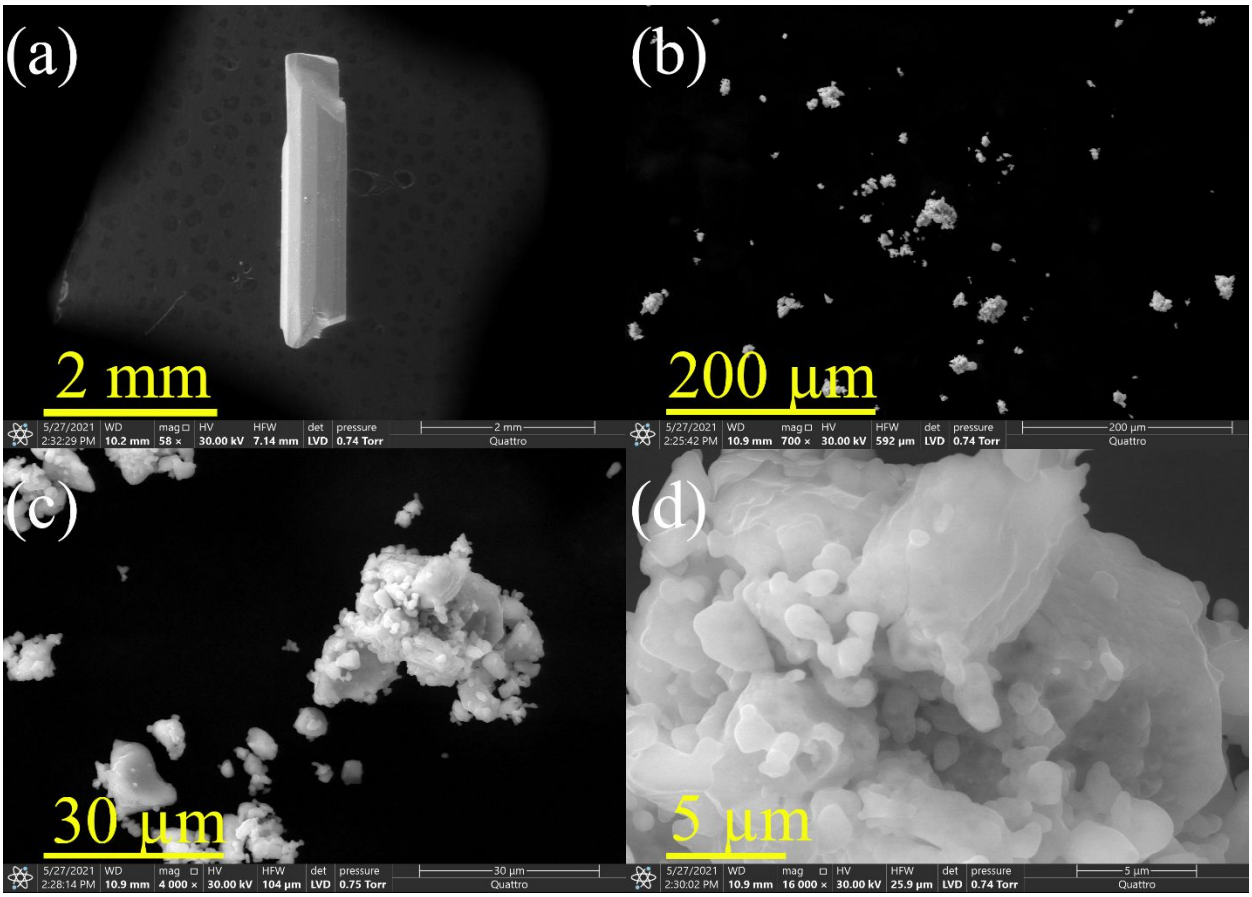

Figure S8. Environmental scanning electron microscope (ESEM) images of (a) a single crystal and (b-d) ground polycrystalline powders of $(NH_4)_2AgI_3$.

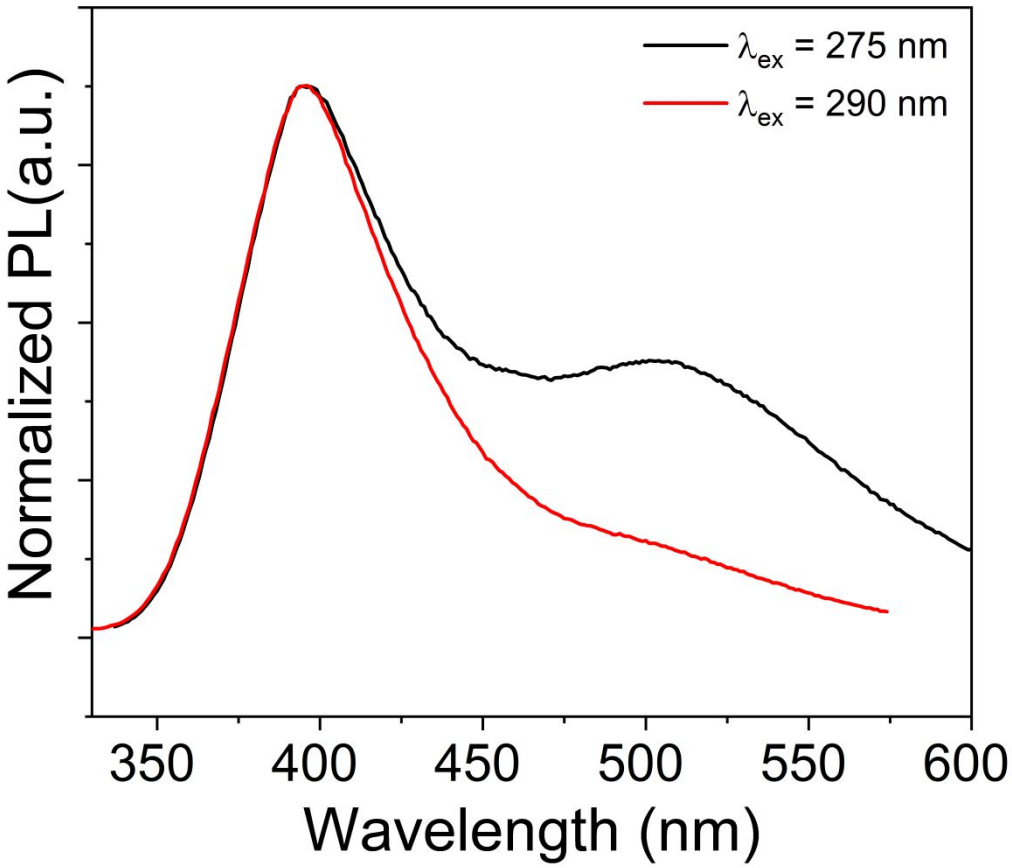

Figure S9. A comparison of PL emission using different excitation energies for $(NH_4)_2AgBr_3$.

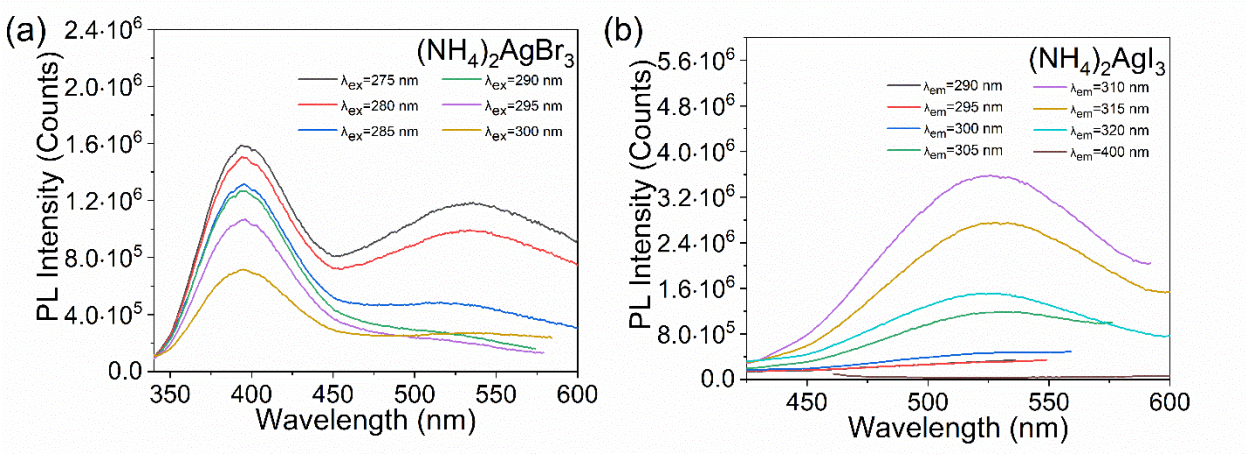

Figure S10. Excitation-dependent PL emission spectra for (a) $(NH_4)_2AgBr_3$ and (b) $(NH_4)_2AgI_3$.